Uncertainties estimation in identification of digital planar surface parameters using a 3D laser sensor

Mohamed Barki and Farid Asma*

Laboratory of Development, Characterization of Materials and Modelling,
Mouloud Mammeri University of Tizi-Ouzou,
BP 17 RP 15000, Tizi-Ouzou, Algeria
Email: barki24@yahoo.fr
Email: asma7farid@yahoo.fr
*Corresponding author

Abstract: In modern metrological applications, 3D laser sensors are used to measure surface parameters. However, the performance of 3D laser sensor is influenced by its position and orientation angles on the target, which causes uncertainties in the measured parameters. In this paper, the influence of the position and orientation of a 3D laser plane sensor is studied by determining the measurement uncertainties on the parameters of a flat surface. Relative position and two orientation angles between the sensor and the surface are taken as the main characteristics of the sensor and are considered separately. In order to determine the uncertainties in the measurements, a set of measurements are performed on a reference part by using a coordinate measuring machine (CMM) equipped with a laser plane sensor.

Keywords: 3D sensor; uncertainties estimation; coordinate measuring machine; CMM.

Reference to this paper should be made as follows: Barki, M. and Asma, F. (2018) 'Uncertainties estimation in identification of digital planar surface parameters using a 3D laser sensor', *Int. J. Quality Engineering and Technology*, Vol. 7, No. 1, pp.82–97.

Biographical notes: Mohamed Barki is a doctoral student at the Mouloud Mammeri University of Tizi-Ouzou. He holds an Engineer degree from the University of Science and Technology Houari Boumediene of Algiers in 2002 and Magister degree from the Polytechnic National School of Algiers in 2008.

Farid Asma is an Associate Professor in the Mechanical Engineering Department at the Mouloud Mammeri University of Tizi-Ouzou. He holds an Engineer degree and Magister degree from the National Institute of Mechnical Engineering in Boumerdès, and PhD degree from the Mouloud Mammeri University of Tizi-Ouzou. He is a member of the research team modelling the behaviour of materials of the Laboratory of Development, Characterization of Materials and Modelling. His research interest includes computer aided modelling, computer aided manufacturing, modelling errors, structural dynamics, and inverse methods.

1 Introduction

The rapid development of manufacturing techniques as CNC machines, machining centres, provides relatively complex surfaces. Therefore, inspection of these parts requires using three-dimensional control instruments. At this level, the use of a coordinate measuring machine (CMM) equipped with a touch trigger probe is necessary to control the geometry of the parts. Unfortunately, the verification that the manufactured part conforms to the specifications of its technical drawing using a CMM is always long and tedious. Thus, the measurement does not provide the customer with added value, the part time control needs therefore to be minimised (Isheil et al., 2011). These factors lead manufacturers to look for other 3D controls. The basic idea is to replace the feelers by contactless sensors that significantly reduce the measurement time. These sensors provide a fast geometric representation of surfaces and volumes as a cloud of points, the result is an image of the part as measured in the form of a digital file rich in information, for analysis of complex surfaces such as curved surfaces. In addition, correction such as that of the probing system in the case of measurement with a CMM contact is no longer necessary. It also allows the measurement of flexible parts, deformable in the case of contact with the probe. Certainly, this technique provides solutions to measurements of engineering parts, however, its accuracy needs improvement due to some factors, such as the reflection of the laser beam, the geometry of the part and its roughness, the position of the sensor relative to the piece.

The errors in measurements can be due to several factors, in particular, intrinsic errors related to metrological parameters of the sensor (these errors are initially corrected by the manufacturer (Fontaine et al., 2005) and others corresponding to the orientation and position of the sensor relative to the measured part.

In the following, three position parameters are considered: two angles α and β orientation of the sensor relative to the work-piece and the distance d between the sensor and the surface to be measured (Figure 1). The study focuses on standard uncertainties following a global approach.

Figure 1 Location parameters α, β and d (see online version for colours)

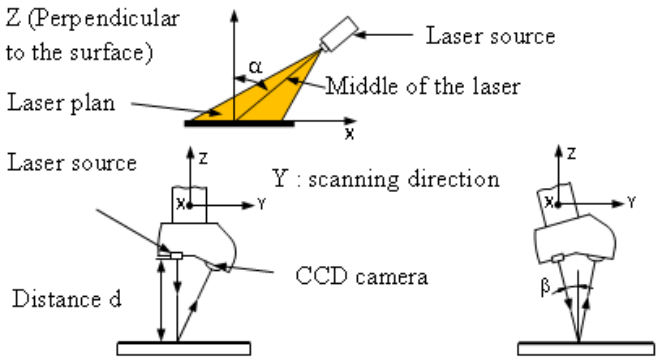

These three parameters have been subject of several works during recent years (Fontaine et al., 2005; Feng et al., 2001; Xi et al., 2001) have studied the evolution of systematic errors on the distance between the centre of a sphere and a plane based on three

parameters. Prieto (1999) studied the variance-covariance matrices according to the three machine axes for each of these parameters. Isheil (2008) has estimated systematic positioning errors which are determined by calculating the distance between two points, each point is defined by the intersection of three planes by considering the distance d. Van Gestel et al. (2009) investigated the influence of three parameters in the case of plane measurement in the context of temperature stabilisation.

This present study focuses on measuring the standard uncertainties due to these same parameters by studying the evolution of uncertainties on coefficients of a plane (overall error) by varying the three considered parameters to determine the optimal configuration for which uncertainty is minimal and the measurement accuracy is improved.

2 Surface scanning with a plane laser sensor

The method for scanning inclined surfaces with a plane laser sensor is the same as 3D measurement with contact measurement system, except the replacement of feelers with laser sensors. The measurement system considered by Mehdi-Souzani et al. (2006) consists of a gantry tiny CMM, an LC50 laser plane sensor whose field of view is a square of 50 mm^2. The sensor is mounted on the Z-axis CMM via a motorised rotating head PH10. This arrangement allows five degrees of freedom to the sensor during scanning the room, respectively three translations along the X, Y and Z axes and two rotations around the Y and Z axes (Isheil et al., 2011; Fontaine et al., 2005). The treatment of cloud of recorded points is performed using a metrologist software. In this work, a MATLAB code is written for the treatment of clouds of points.

During a measurement, different error sources act significantly on the measurement uncertainty. Some may be considered having negligible effects, such as machine-related errors (guides are considered perfect and associated axes orthogonal). Other errors can be reduced such as those due to physical characteristics (roughness, reflectivity). The position of the sensor relative to the piece also affects the measurement results and can be considered as a source of significant errors (Bouaziz et al., 2011). Prieto (1999) defines the extrinsic parameters characterising the position of the laser sensor: the distance from the sensor to the part, the angle of incidence α in the plane of laser and the ortho-incidence angle β in the perpendicular plane to the laser plane.

3 Modelling of measurement uncertainties

The formal definition of the term ‘measurement uncertainty’ adopted by the international vocabulary of metrology (IVM) (Article 3.9, JCGM, 2008) is: *Parameter associated with the result of a measurement that characterises the dispersion of values that could reasonably be attributed to the measurand. This parameter may be for example, a standard deviation (or a multiple of it) or the half width of an interval having a stated level of confidence*. The standard [NF X07-020 96] provides two procedures for quantifying uncertainties in measurement uncertainties. The first, called type A, described as statistical method based on a series of measurements. The second, called type B, based on data from manufacturer's specification, calibration certificate, uncertainty assigned, etc. (JCGM, 2008). In this work, the method is of type A.

3.1 Modelling by global approach

Identifying curve or surface parameters from a cloud of points is a very common problem in science and engineering. This lead to a mathematical equation of a surface or a curve based on real data. Many studies (Bourdet, 1987; Mathieu, 1997) carried on this problem have used standard least square algorithms assuming that the coordinates of the recorded points are not vitiated by errors (their distribution is assumed to be zero variance). However, these authors are most often limited to estimate geometrical parameters without associated uncertainty. In Abdelilah et al. (2015), the authors considered that the coordinates of the recorded points are tainted with errors and determined the uncertainties associated with the geometrical parameters in the case of the measurement with contact.

The present article aims to study the uncertainty evolution of each coefficient of the equation of a plane, in contactless measurement. This uncertainty is based on sensor/piece position. To do this, a laser scanning of the reference part is performed several times.

3.2 Mathematical formulation

3D points recorded by the CCD camera do not really belong to the measured part, they are tainted with errors, but it is possible to make the correspondence between them using the concept of uncertainty, allowing to write for a point, Prieto (1999):

$$\left(x_{mes}, y_{mes}, z_{mes}\right) = (x, y, z) \pm U(x, y, z) \tag{1}$$

where

$(x_{mes}, y_{mes}, z_{mes})$ are coordinates measured from a surveyed point.

(x, y, z) are actual coordinates of a surveyed point.

$U(x, y, z)$ is the uncertainty around a surveyed point.

In 3D metrology, a measured point M is defined by its Cartesian coordinates (Mx, My, Mz) in a given landmark and its uncertainty U_M (U_{Mx}, U_{My}, U_{Mz}) (Bachmann et al., 2004).

From statistical methods JCGM (2008), we can assume that the conventionally real coordinates of the point M are evaluated by their mathematical expectation. From where:

$$Mx = E\left[Mx_{mes}\right], My = \left[My_{mes}\right], Mz = E\left[Mz_{mes}\right] \tag{2}$$

with:

$$\begin{aligned} &E\left[Mx_{mes}\right] = (1/n)\sum_{i=1}^{n} xi_{mes}, E\left[My_{mes}\right] = (1/n)\sum_{i=1}^{n} yi_{mes}, \\ &E\left[Mz_{mes}\right] = (1/n)\sum_{i=1}^{n} zi_{mes} \end{aligned} \tag{3}$$

Uncertainties: U_{Mx}, U_{My} and U_{Mz} are determined from the following formulas:

$$U_{Mx} = k\sigma_{Mx}; U_{My} = k\sigma_{My}; U_{Mz} = k\sigma_{Mz} \tag{4}$$

k is the enlargement factor chosen according to the measurement conditions and depends on the probability desired (generally k = 2 corresponding to a probability of about 95% if the variation follows a Gaussian distribution).

σ_{Mx}, σ_{My}, σ_{Mz}, are the estimated standard deviations for (x_{mes},y_{mes},z_{mes}), such as:

$$\sigma_{Mx} = \sqrt{\frac{\sum_{i=1}^{n}\left(Mxi_{mes} - Mx\right)^2}{n-1}}, \sigma_{My} = \sqrt{\frac{\sum_{i=1}^{n}\left(Myi_{mes} - My\right)^2}{n-1}}, \quad \sigma_{Mz} = \sqrt{\frac{\sum_{i=1}^{n}\left(Mzi_{mes} - Mz\right)^2}{n-1}} \tag{5}$$

This article presents the influence of the same parameters on the coefficients of a plane; the uncertainty of a point is no longer necessary because the geometric control is global (roundness, flatness, …). On the other hand, digitisation always results in the discontinuous representation of a surface as a cloud of points and it is difficult to apply the expression of uncertainty in measurement at each point.

3.3 Determination of the flat surface parameters and estimation of their uncertainties

In an orthonormal landmark, every plane P has an equation of form: a.x+b.y + c.z+d = 0 with a, b and c not zero. This lead to:

$$z = Ax + By + C \tag{6}$$

The ordinary least squares method used to optimise a plane consists in determining the coefficients A, B and C. The laser planar sensor converts the measured part into a cloud of points. For a point Mi (x_i, y_i, z_i) belonging to the cloud of points and not belonging to the plane z = Ax + By + C, z can be expressed as

$$z_i = Ax_i + By_i + C + e_i \tag{7}$$

From where:

$$e_i = z_i - \left(Ax_i + By_i + C\right) \tag{8}$$

Let the function

$$S(A, B, C) = \sum_{i=1}^{n} e_i^2 = \sum_{i=1}^{n}\left(z_i - \left(A.x_i + B.y_i + C\right)\right)^2 \tag{9}$$

According to Bourdet (1987), e_i can be considered as perpendicular to the plane P, because the difference between perpendicular and vertical error e_i is very small, this introduces a very small default, which is not involved in the Metrology of mechanical parts. The coefficients A, B, and C are determined by minimising the function S using to the least square method

$$\frac{\partial S}{\partial A} = \frac{\partial S}{\partial B} = \frac{\partial S}{\partial C} = 0 \tag{10}$$

The values of A, B, C of each digitisation are obtained by:

$$\begin{bmatrix} A_j \\ B_j \\ C_j \end{bmatrix} = \begin{bmatrix} \sum_i^n x_{ij}^2 & \sum_i^n x_{ij}y_{ij} & \sum_i^n x_{ij} \\ \sum_i^n x_{ij}y_{ij} & \sum_i^n y_{ij}^2 & \sum_i^n y_{ij} \\ \sum_i^n x_{ij} & \sum_i^n y_{ij} & n_j \end{bmatrix}^{-1} \cdot \begin{bmatrix} \sum_i^n x_{ij}z_{ij} \\ \sum_i^n y_{ij}z_{ij} \\ \sum_i^n z_{ij} \end{bmatrix} \quad j: 1, \ldots, m \tag{11}$$

The index j represents the scanning operation number; it varies from 1 to m, where m is the total number of performed scans.

Obviously, the uncertainties associated with each point recorded during the scanning of the parts, causing uncertainty in the coefficients of a plane, these are also dependent on the laser sensor configuration.

In order to determine the average values of coefficients A, B, C, and assess their associated uncertainties U_A, U_B, U_C, it is necessary to make m measurement with $m \geq 5$ according to the GPS standard. In this study, m is taken as m = 5.

Finally,

$$\begin{aligned} &A_{moy} = (1/m)\sum_{k=1}^{m} A_k,\ B_{moy} = (1/m)\sum_{k=1}^{m} B_k, \\ &C_{moy} = (1/m)\sum_{k=1}^{m} C_k \end{aligned} \tag{12}$$

$$\begin{aligned} &U_A = k.\sqrt{\frac{\sum_{k=1}^{m}(A_k - A_{moy})^2}{m-1}},\ U_B = k.\sqrt{\frac{\sum_{k=1}^{m}(B_k - B_{moy})^2}{m-1}}, \\ &U_C = k.\sqrt{\frac{\sum_{k=1}^{m}(C_k - C_{moy})^2}{m-1}}, \end{aligned} \tag{13}$$

According to Bourdet (1987) the correct writing of a value evaluated using a series of measurements is:

$$A = A_{moy} \pm U_A,\ B = B_{moy} \pm U_B,\ C = C_{moy} \pm U_C \tag{14}$$

Hence the influence of the sensor/part position parameters is:

$$\begin{aligned} &A = A_{moy}(\alpha, \beta, d) + U_A(\alpha, \beta, d);\ B = B_{moy}(\alpha, \beta, d) + U_B(\alpha, \beta, d); \\ &C = C_{moy}(\alpha, \beta, d) + U_C(\alpha, \beta, d) \end{aligned}$$

Such as A, B, and C represent the desired coefficients of a theoretical plane, and A_{moy}, B_{moy}, and C_{moy} are the corresponding average values respectively and conventionally considered true, JCGM (2008).

U_A, U_B, U_C: expanded uncertainties associated with coefficients A, B, and C, respectively.

4 Experimental section

In order to determine the conventionally true values of the coefficients of a flat surface, and estimate their uncertainties based on the sensor/part position, measurements are performed using a CMM fitted with a LC50 on a reference piece called triplane artefact (truncated pyramid) (Figure 2). This part is made of a reconstituted wood, Ra ≅ 4.8 µm, a material with a matte surface suitable for laser measurement (Fontaine et al., 2005).

Figure 2 The triplane artefact (see online version for colours)

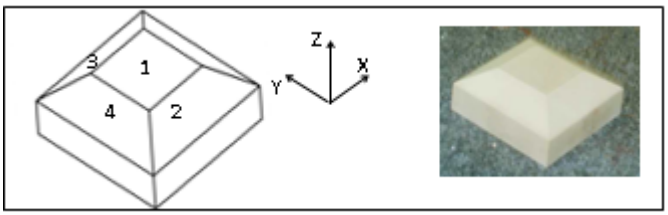

The choice of the triplane artefact as reference piece is related to its geometry, Contri (2002). This part presents the intersection of three non-orthogonal planes so we can have a clear idea of the influence of the geometry, this piece also presents the need to use the CMM for the determination of the distance between the two intersection points of the planes 1, 2 and 4 with the planes 1, 3 and 4. After sensor calibration phase, scanning is performed on all the planes.

The planes 2, 3 and 4 are inclined by 30º to the horizontal. The part is arranged so that the plane 4 is in the scanning direction, and the plane 1 parallel to the marble of the CMM, which is considered as a reference surface. The sensor is maintained in a given configuration. For each parameter, α, β and d, a series of scans of the artefact are performed, the total number of scans made is 120, 35 scans varying α, 35 scans varying β, and 50 scans varying d.

The scans according to the parameters considered are spaced in time and carried out with a constant speed to eliminate any uncertainty caused by the acceleration.

4.1 Scanning varying parameter α

In these tests, the parameters β and d are fixed to β = 0º and d = 125 mm (the distance d is given according to the calibration of the sensor). The angle α varies from 0º to 45º by a step of 7.5º (Figure 3). For each laser scanning, the number of recorded points is approximately 20000.

Figure 3 Different orientations of the sensor according to the angle α (see online version for colours)

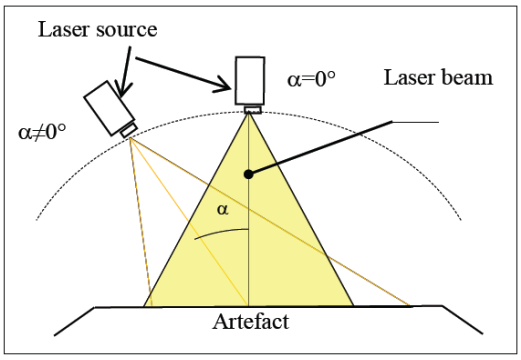

4.2 Scanning varying parameter β

In these digitalisations, the same variation is followed for the angle β, the other two parameters are kept fixed: α = 0º and d = 125 mm. The CMM scanning system equipped with a laser sensor does not ensure changes in the β angle (β set to 0º). To study the influence of the variation, a device inspired by Isheil (2008) is used, (Figure 4).

In the tests, the angle β varies from –30º to +30º by a step of 10º. For β = –30º, the laser plane is perpendicular to plane 2, and for β = 30º it is perpendicular to plane 3.

Figure 4 Mounting device for the variation of the angle β

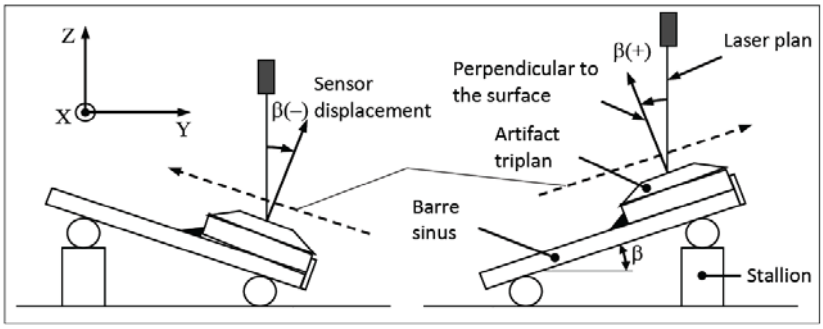

Figure 5 Variation of parameter d (see online version for colours)

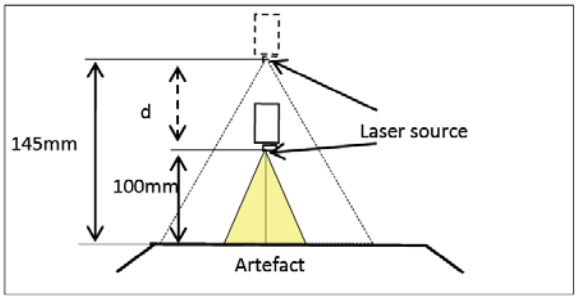

4.3 Scanning according to parameter d

The variation of d is obtained by a displacement along the Z axis of the sensor in the space of the CMM. In this part, α and β are maintained α = 0º, β = 0º and d was varied from 100 to 145 mm by 5 mm step (Figure 5). The number of points recorded in each scan is as before, approximately 20000 points.

5 Results and discussions

The tests generated a digital files witch represent the clouds of points recorded by the CCD camera when scanning artefact. To explore these clouds of points, calculation codes under MATLAB are implemented. These codes allow the visualisation, segmentation and optimisation of the four planes (Figure 6) and then the determination of the measurement uncertainties associated with each coefficient versus the considered parameters.

Figure 6 Treatment of the cloud of points

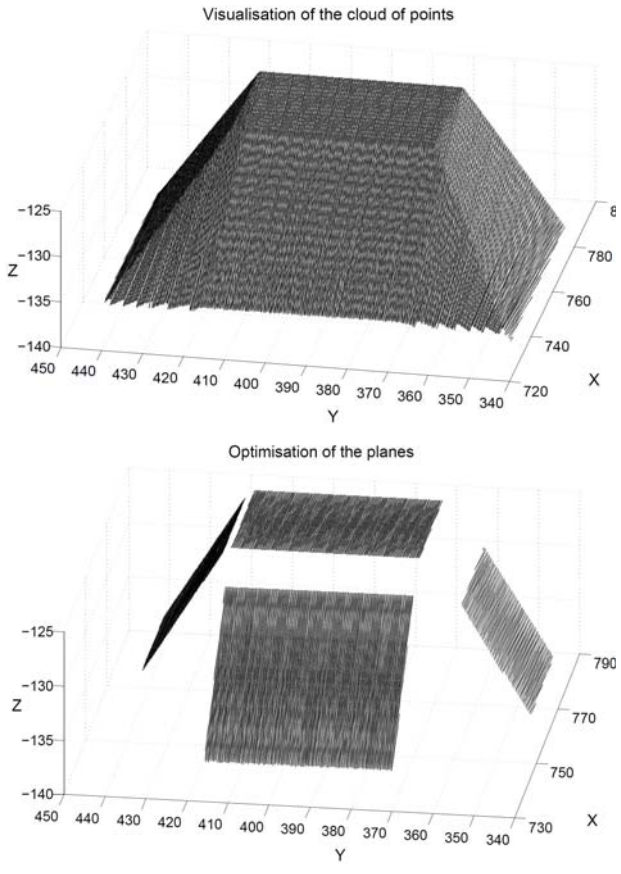

Notes: Visualisation, optimisation.

5.1 Influence of the parameter α

This section presents the evolution of the measurement uncertainty of the coefficient C, $U_C(\alpha, \beta, d)$ for the four planes. According to the results obtained, $U_A(\alpha, \beta, d)$ and $U_B(\alpha, \beta, d)$ are very small compared to $U_C(\alpha, \beta, d)$ (Table 1).

Table 1 summarises the results obtained for the configuration $\alpha = 30°$, $\beta = 0°$ and $d = 125$ mm.

Table 1 Dispersion of coefficients A, B, and C of the optimal planes of the triplane artefact

α = 30°, β = 0°, d = 125 mm	U_A	U_B	U_C
Plane 1	$0{,}0020.10^{-2}$	$0{,}0054.10^{-2}$	$2{,}9820.10^{-2}$
Plane 2	$0{,}0046.10^{-2}$	$0{,}0080.10^{-2}$	$3{,}6722.10^{-2}$
Plane 3	$0{,}0054.10^{-2}$	$0{,}0130.10^{-2}$	$7{,}6162.10^{-2}$
Plane 4	$0{,}0054.10^{-2}$	$0{,}0068.10^{-2}$	$5{,}0360.10^{-2}$

Figure 7 illustrates the variation of $U_C(\alpha)$ uncertainty of the four planes. The variation of $U_C(\alpha)$ is approximated by a straight line.

Figure 7 Variation of the uncertainty coefficient U_C versus the angle α

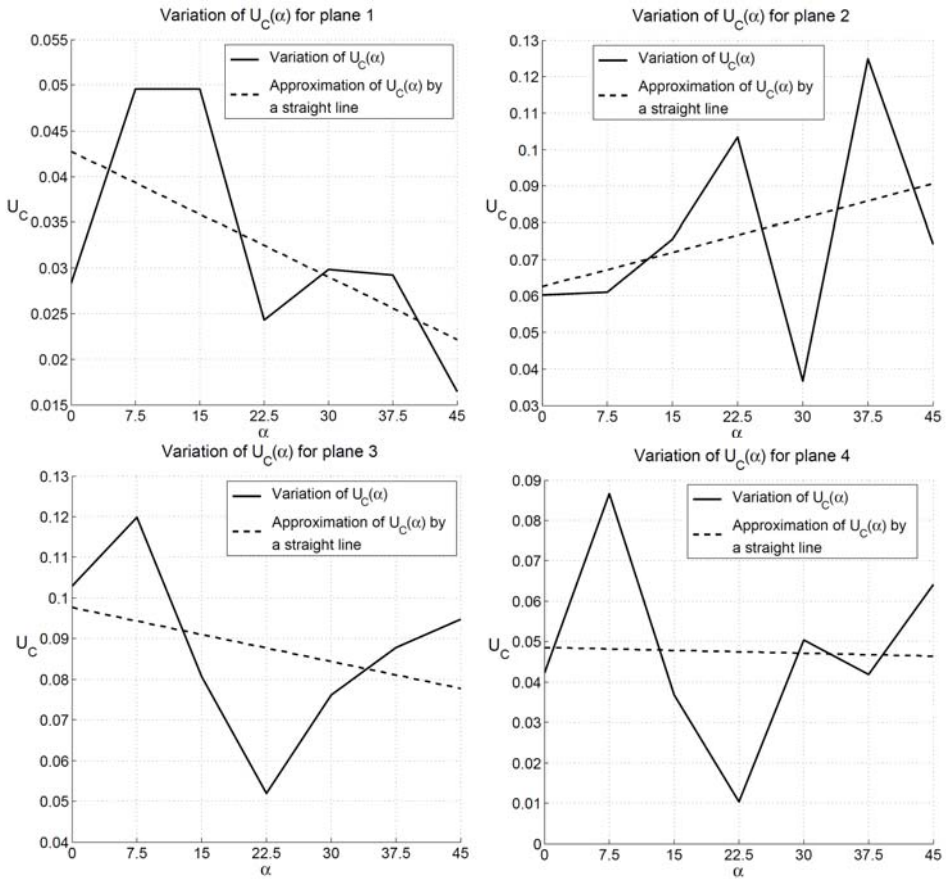

From Figure 7, it can be seen that U_C decreases when α increases for planes 1 and 3, and when α increases U_C increases for plane 2. For plane 4 $U_C(\alpha)$ is almost constant, this can be explained by the variation in the number of points recorded on each plane. When the angle α increases the number of recorded points increases, but in the case of plane 2 the U_C increases due to considerable shape defects in this plane: 39.6 µm.

Note that the dispersion of $U_C(\alpha)$ of the planes 2 and 3 is approximately 10 times greater than $U_C(\alpha)$ of the planes 1 and 4. This can be due to the number of points recorded on each plane and the effect of the part geometry for the planes 2 and 3 because the laser plane orthogonal to the planes 1 and 4 during digitisation is inclined by 30º for planes 2 and 3, suggesting an orthogonal orientation of the sensor during digitisation. These results are consistent with the results presented by Prieto (1999) for a measured point.

5.2 Influence of the parameter β

Figure 8 illustrates the variation of $U_C(\beta)$ uncertainty of the four planes.

Figure 8 Variation of the uncertainty coefficient U_C versus the angle β

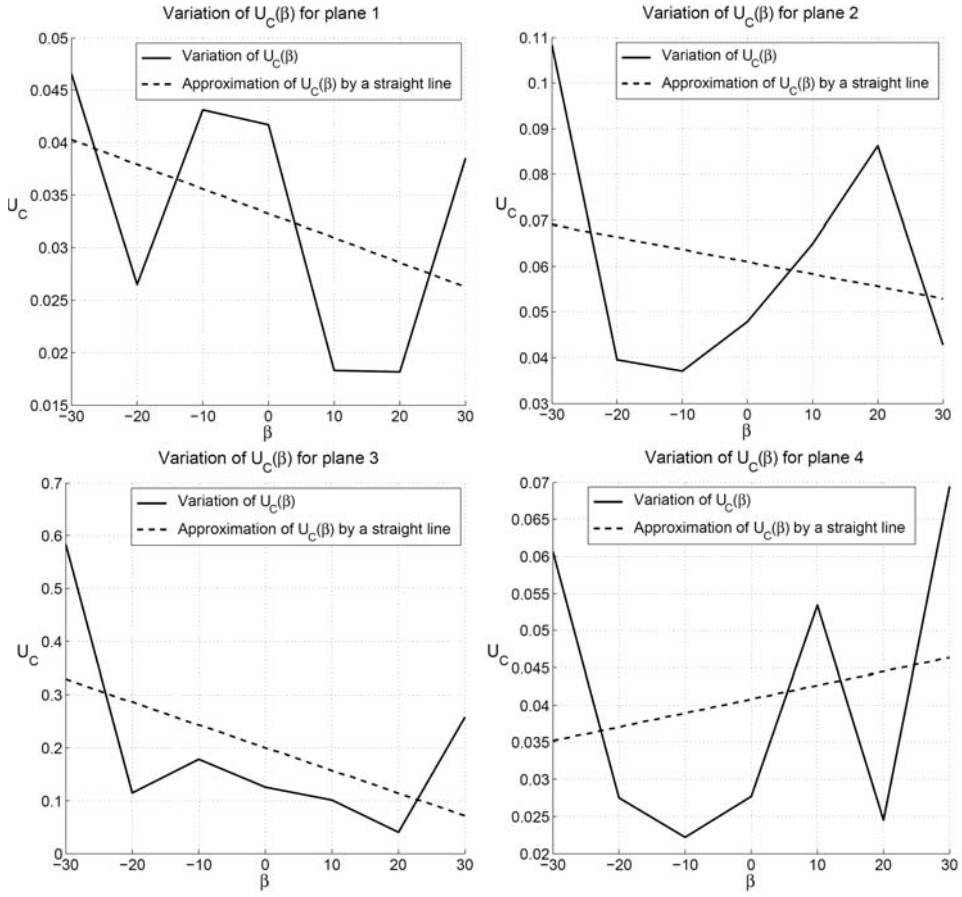

The curves of Figure 8 show that the uncertainty $U_C(\beta)$ decreases with the variation of the β angle from –30º to 30º for planes 1, 2 and 3, and increases for plane 4. The largest dispersion is recorded in planes 2 and 3, $0.05 \leq U_C(\beta) \leq 0.584$, as well as the largest uncertainty is recorded on plane 3 (0.584), whereas, the smallest dispersion is recorded in planes 1 and 4, $0.018 \leq U_C(\beta) \leq 0.046$. All this, can be explained as follows: when $\beta = -30º$, the laser plane is perpendicular to plane 2, for this position, the number of points on this plane is maximal. When $\beta = +30º$, the laser plane becomes perpendicular to the plane 3 and the number of points recorded on this plane is maximal. As for the number of points recorded on plane 4, it is almost constant as well as on plane 1 since the sensor moves parallel to plane 1.

The large dispersion of the values of U_C in the planes 3 and 2 is also explained by the effect of the geometry of the part, which subsequently causes physical distortions. Note that for $\beta = -30º$ the plane 3 is at 60º to the horizontal, in this case the number of points recorded on this plane greatly reduced the effect of the reflection of the laser plane.

Figure 9 Variation of U_C uncertainty coefficient versus the distance d

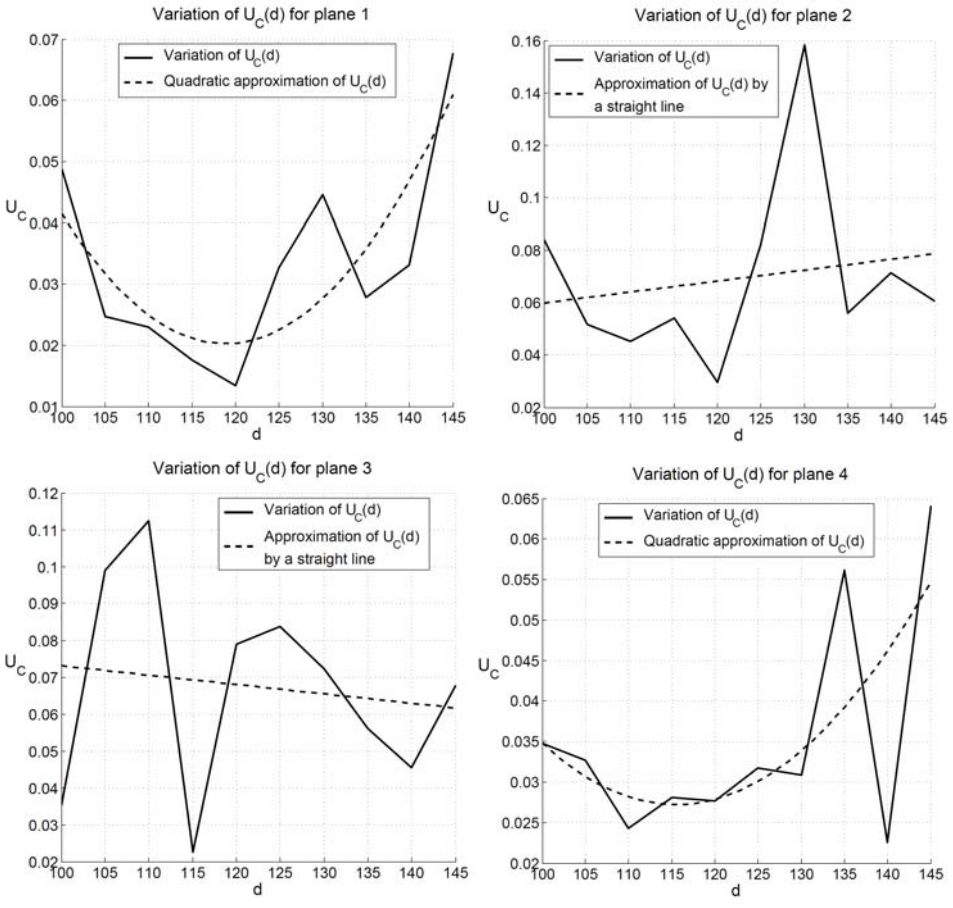

5.3 Influence of the parameter d

Figure 9 illustrates the variation of $U_C(d)$ uncertainty of the four planes.

From the curves and its approximation by a straight line in Figure 9, it can be seen that $U_C(d)$ increases as d increases for plane 2 and decreases for plane 3. For the planes 1 and 4, the approximation of the variation of $U_C(d)$ by a second order polynomial for the plane 1 shows that $U_C(d)$ decreases when d varies from 100 to 120 mm and increases when it varies from 120 to 145 mm. The plane 4 shows that $U_C(d)$ decreases when d varies from 100 to 115mm and increases when it varies from 115 to 145 mm. The largest dispersion is recorded on the planes 2 and 3, this can be explained by the number of points recorded on each plane. Generally, the number of recorded points decreases when the distance increases (the planes become less visible, especially the inclined ones). The best results are recorded around the focal distance of the sensor $115 \leq d \leq 135$ mm.

5.4 Determination of relative uncertainties

The results above show that U_C uncertainty is greater than U_A and U_B, because the coefficients A and B represent the optimal slopes of inclination of the planes according to planes XOY, YOZ respectively. In addition, coefficient C represents the intersection of the optimal planes with the Z-axis, then the coefficient C is greater than A and B coefficients, this led to U_C greater than U_A and U_B, so the results depend on the chosen landmark. These results also show that U_C increases slightly with the increase of C. To get a clear idea the notion of relative uncertainty is introduced, from where:

$$U_{RA} = \left|\frac{U_A}{A_{moy}}\right|; U_{RB} = \left|\frac{U_B}{B_{moy}}\right|; U_{RC} = \left|\frac{U_C}{C_{moy}}\right| \tag{15}$$

Figure 10 illustrates the variations of the relative uncertainties $U_{RA}(\alpha, \beta, d)$ and $U_{RB}(\alpha, \beta, d)$ of plane 1 of the triplane artefact.

Generally, the influence of the position parameters of the laser sensor on the uncertainties of a flat surface are low ($U_A < 0.08.A$, $U_B < 0.05.B$, $U_C < 0.008.C$), in particular for the inclined planes. These uncertainties cannot be neglected, because for large parts or parts that have a narrow tolerance range, the defect control of a flat surface requires the use of the complete theoretical plane equation, therefore all uncertainties $U_A(\alpha, \beta, d)$, $U_B(\alpha, \beta, d)$, $U_C(\alpha, \beta, d)$ act on the shape defect evaluation.

A similar trend is observed on figure 10, for the relative uncertainties $U_{RA}(\alpha, \beta, d)$, $U_{RB}(\alpha, \beta, d)$ and $U_C(\alpha, \beta, d)$, the largest dispersion corresponds the coefficient A, the effect of α is ten times greater than the effect of d and β. When $\beta = 0^o$, $U_{RA}(\beta)$ and $U_{RB}(\beta)$ reach their peak values. As a result, the reliability of the digitisation of the surface is achieved, because for $\beta = 0^o$ plane 1 is parallel to the marble of the CMM, therefore the coefficient A and B are closer to zero, which increases U_{RA} and U_{RB}.

It can be seen that the uncertainty $U_C(\alpha, \beta, d)$ of the plane 1 is smaller to that of the other planes, in particular, in plane 2 and 3, this can be explained by the number of points recorded on this plane and by the geometry of the part.

As shown in Figures 7 to 10, the relative uncertainties U_C, U_{RA} and U_{RB} are random variables, and therfore it is difficult to model and predict their variation.

Finally, for each plane and each parameter α, β, and d an optimum scanning position can be defined.

Figure 10 Variation of the relative uncertainties U_{RA} and U_{RB} versus α, β, and d for plane 1

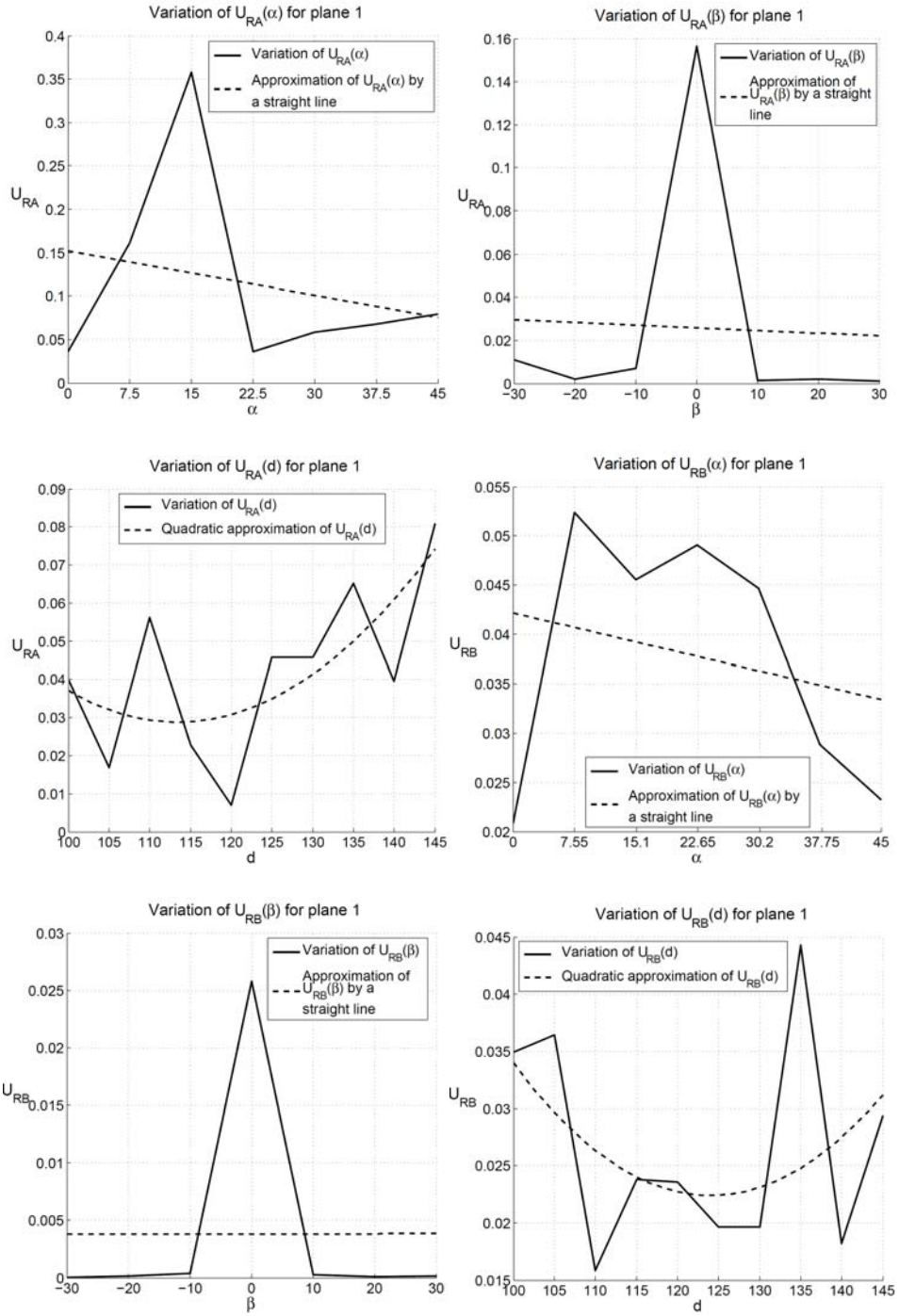

6 Conclusions

In this work, the influence of the position and orientation of a laser sensor on the measurement uncertainties associated with the parameters of a flat surface is studied. The results obtained show that the evolution of the standard uncertainty of each coefficient A, B and C as a function of the three parameters of position and orientation is generally of a few hundredths of each coefficient, and a few tenths for some configurations. Configurations corresponding to the minimum uncertainties can be defined. It is also observed that the shape defects influence the standard uncertainties, more important they are, the more these uncertainties are significant (plane 2). It is also observed that the geometry of the part to be inspected influences the rate of the number of recorded points (case of planes 2 and 3), when the number of points decreases the uncertainty increases. Contrary to what was thought, the laser scanning appears to be more accurate, in particular for parts which have a non-negligible shape defect; this can be explained by the density of points obtained by scanning which allow taking better account of them. It remains to solve the influence of some physical parameters such as the reflection of shiny surfaces, the part geometry and surface roughness.

CMM with a laser sensor performs rapid measurements of engineering parts with less reflective surfaces and with common precision. The measurement quality using this machine can be improved by choosing an optimum position defined by the configuration of the three laser sensor parameters relatively to the part to be measured.

References

Abdelilah, J., Hariri, S. and Senelaer, J-P. (2015) 'Estimation of form deviation and the associated uncertainty in coordinate metrology', *International Journal of Quality and Reliability Management*, Vol. 32, No. 5, pp.465–471.

Bachmann, J., Linares, J.M., Sprauel, J.M. and Bourdet, P. (2004) 'Aide in decision-making: contribution to uncertainties in three-dimensional measurement', *Precision Engineering*, Vol. 28, No. 1, pp.78-88, DOI: 10.1016/S0141-6359(03)00079-5.

Bouaziz, M., Barki, M., Isheil, A. and Fontaine, J.F. (2011) 'Etude de l'influence de l'orientation d'un capteur de mesure a nappe plan laser sur les incertitudes de mesure en 3D', *15th International Congress of Metrology*, Paris, France.

Bourdet, P. (1987) *Contribution to Three-Dimensional Measurement: Geometric Surface Identification Model, Functional Metrology of Mechanical Parts, Geometric Correction of Coordinate Measuring Machines*, PhD thesis, Nancy 1 University, France.

Contri, A. (2002) *Geometric Quality of the Measurement of Complex Surfaces by Optical Means*, PhD thesis, ENS Cachan, France.

Feng, H.Y., Liu, Y. and Xi, F. (2001) 'Analysis of digitizing errors of a laser scanning system', *Precision Engineering*, Vol. 25, No. 3, pp.185–191, DOI: 10.1016/S0141-6359(00)00071-4.

Fontaine, J.F., Gonnet, J.P., Isheil, A. and Joannic, D. (2005) 'Parameters analysis influencing 3D measurement without contact by laser scanner to make a compensation model', *9th CAT CIRP Seminar*, France.

Isheil, A. (2008) *Analysis and Correction of the Errors of a 3D Non-Contact Laser-Based Sensor*, PhD thesis, Université de Bourgogne, France.

Isheil, A., Gonnet, J.P., Joannic, D. and Fontaine, J.F. (2011) 'Systematic error correction of a 3D laser scanning measurement device', *Optics and Laser in Engineering*, Vol. 49, No. 1, pp.16–24, DOI: 10.1016/j.optlaseng.2010.09.006.

JCGM (2008) 'Evaluation of measurement data – guide to the expression of uncertainty in measurement', *Joint Committee for Guides in Metrology*.

Mathieu, L. (1997) 'Nouvel algorithme pour la vérification sur MMT des spécifications géométriques normalisées', *8th International Congress of Metrology*, Besançon, France.

Mehdi-Souzani, C., Thiébaut, F. and Lartigue, C. (2006) 'Scan planning strategy for a general digitized surface', *Journal of Computing and Information Science in Engineering*, Vol. 6, No. 4, pp.331–339, DOI: 10.1115/1.2353853.

Prieto, F. (1999) *Computer-Assisted Metrology. Contribution of 3D Contactless Sensors*, PhD Thesis, INSA, Lyon, France.

Van Gestel, N., Cuypers, S., Bleys, P. and Kruth, J-P. (2009) 'A performance evaluation test for laser line scanners on CMMs', *Optics and Lasers in Engineering*, Vol. 47, Nos. 3–4, pp.336–342, DOI: 10.1016/j.optlaseng.2008.06.001.

Xi, F., Liu, Y. and Feng, H-Y. (2001) 'Error compensation for three-dimensional line laser scanning data', *International Journal of Advanced Manufacturing Technology*, Vol. 18, No. 3, pp.211–216, DOI: 10.1007/s001700170076.